Heterogeneity effects on nondestructive assay measurements of enrichment in UF$_6$ cylinders

Allison T. Greaney[1], Susan K. Smith[1], Ramkumar Venkataraman[1], Jason M. Richards[1], Carlos D. Rael[2], Martyn T. Swinhoe[2], Duc T. Vo[2], Ron D. Jeffcoat[3], and Glenn A. Fugate[1],

[1]Oak Ridge National Laboratory, Oak Ridge, TN 37831, USA
[2]Los Alamos National Laboratory, Los Alamos, NM 87545, USA
[3]Savannah River National Laboratory, Aiken, SC 29808, USA
E-mail: fugatega@ornl.gov

Abstract

Measurements were performed using multiple mechanically cooled high-purity germanium detectors at six positions around standard industrial 30B cylinders (2.2 metric ton) of UF$_6$ to assess if matrix inhomogeneity is detectable and its impacts on the measured apparent uranium enrichment. Uranium enrichment was calculated with FRAM™. Six of the nine cylinders appeared to be homogeneous as indicated by having similarly accurate apparent measured uranium enrichment, at all positions. However, three cylinders appeared to have localized inhomogeneities. This was manifested as very low apparent enrichments, often <10% of the declared value, on one side of the cylinder. Examination of the spectra suggested both elevated ^{234}Th-^{234m}Pa daughter isotopes and reduced ^{235}U were measured at these locations. It is hypothesized that these heterogeneous cylinders may have experienced asymmetric solar heating, which caused volatile UF$_6$ to sublime preferentially away from the warmed side. Care should be taken during uranium enrichment verification when applying methods that include gamma-rays associated with daughter nuclides to the determination of uranium enrichment for cylinders that are stored in sunlight.

Keywords: enrichment; UF$_6$; HPGe; FRAM; spectrometry

1.   Introduction

Accurate quantification of uranium enrichment in uranium hexafluoride (UF$_6$) cylinders is necessary for material accounting and nuclear safeguards. Non-destructive assay (NDA) methods using gamma-ray spectroscopy are often used to verify enrichment declarations. NDA enrichment determinations either employ only the 185.7 keV emission associated with the ^{235}U (e.g., the enrichment meter) or ratios of gamma-ray emissions associated with the radioactive daughter nuclides of one or more uranium isotopes. The Fixed Energy Response Function Analysis with Multiple Efficiency (FRAM™) code can perform isotopic analysis on uranium using gamma- and X-ray peaks associated with ^{234}U, ^{235}U, ^{238}U, and ^{234m}Pa.[1] While more complex, use of FRAM™ eliminates the need for measuring the wall thickness of the cylinder or calibrations using known enrichment uranium materials. For low-enriched uranium

(LEU) analysis, the software can be run in two modes: "planar" which uses 60 – 250 keV peaks and "coaxial" mode which uses 120 – 1010 keV peaks.[2,3,4] The latter mode is useful for applications to thick-walled walled vessels such as standard industrial 30B cylinders (2.2 metric ton) of UF$_6$. For an accurate uranium enrichment to be calculated by FRAM™ or any other method that utilizes gamma-ray emissions from uranium daughter products, the UF$_6$ must be homogenously distributed with respect to uranium and daughter products, and the ^{234}Th and ^{234m}Pa isotopes must be in secular equilibrium with their parent ^{238}U. Given that the half-lives of ^{234}Th and ^{234m}Pa are 24.1 days and 1.17 minutes, respectively, the sample must be at least 3.5 months old (~95% of secular equilibrium) to allow the system to minimize the effects of disequilibrium on the measurement.

The detector geometry, in relation to the distribution of the UF$_6$ inside the cylinder, is also important for accurate analysis. Depending on the manner in which the cylinder was filled, the UF$_6$ may be found in different wall thickness distributions. Initially, gas transfers of UF$_6$ tend to fill with a central void as material sublimes into the cylinder. Liquid filled cylinders initially have a void in the top horizontal half of the cylinder due to volume reduction as the liquid freezes into the denser solid. It should be noted that these are initial geometries which likely progress toward an intermediate state through sublimation and mechanical fracturing over some variable time frame where all surfaces have a significant thickness of UF$_6$ and the large void is predominantly found in the top half of the cylinder. The distribution of UF$_6$ around a full cylinder likely meets the ~1 cm infinite thickness requirement of the 185.7 keV gamma-ray for the enrichment meter method at almost any point. Theoretically, enrichment meter and FRAM™ do not require an infinite thickness for higher energy peaks (e.g. ^{234m}Pa) and so do not need an infinite thickness of UF$_6$. Berndt et al. [5] demonstrated that the detector location and filling profile influence the detector response, and therefore the accuracy of the enrichment, as measured by the enrichment meter measurement. As such, the detector positions were chosen to "guarantee" the requirement of infinite thickness by focusing on the bottom third of the cylinder. Other studies have recently investigated localized spatial impacts related to heel and daughter distribution on spectra and enrichment measurements.

This study presents position-dependent gamma-ray measurements of 30B cylinders made with high purity germanium (HPGe) detectors and analyzed using FRAM™ v5.2 distributed by ORTEC® to determine the uranium enrichment. This approach has been shown to produces quick, accurate results comparable to those of the traditional enrichment meter method [2,6] and has the added advantages that it does not require determination of the wall thickness of the vessel, calibration on a known enrichment uranium material, or an infinite thickness type geometry. This work focused on determining the impacts on enrichment as determined by FRAM™ due to potentially variability within the physical UF_6 distribution and daughter nuclide distribution around the cylinder by performing horizontal profiling.

2. Methods

Gamma-ray spectra were collected around nine 30B UF_6 cylinders that ranged in enrichment between 0.71 and 4.95 weight% ^{235}U. Examination of various enrichment calculation methods [6] and neutron emission rates [7] measurements of these data have been reported elsewhere. The spectra were collected in six positions around the cylinder using commercial, mechanically cooled high purity germanium (HPGe) detectors (**Fig. 1**). These positions were selected to attempt to produce a uniform geometry that assumed a homogenous distribution of uranium and daughter products inside the cylinder without collimation. Both coaxial (three detectors; all ORTEC® portable HPGe detectors) and planar (two detectors; both Canberra/Mirion Falcon 5000 HPGe detectors) crystal types were used. A 10 to 30 minute spectrum was collected using each detector at all six positions around the cylinder (e.g., 5 detectors × 6 positions = 30 gamma-ray spectra per cylinder). The position numbering system was kept constant across all cylinders: positions 1, 2, and 3 were on one side of the cylinder while position 4, 5, and 6 were on the other side (**Fig. 1**). Three of the detectors

were angled so that they were in contact with the face of the cylinder near the base where the suspected UF_6 profile was thickest. The two coaxial detectors had to be positioned in a similar geometry but 12 inches from the wall of the cylinder to decrease the overall deadtime of the measurement. Deadtimes varied between 20% and 90%, with high dead times are addressed in section 4.2. The data were initially collected to examine the full gamma-ray spectrum of each cylinder and so the methodology was not optimized for enrichment measurement purposes, *e.g.,* no collimation was used which may have improved the measurement.

The gamma-ray spectra were analyzed with the commercial FRAM™ software in "coaxial" mode, using the ULEU_Cx_120-1010 parameter set. Using this parameter set, the software uses ratios of high and low energy peaks to quantify the isotopic fractions of ^{234}U, ^{235}U, ^{236}U, and ^{238}U. The ^{235}U enrichment is calculated using a ratio between the 185.7 keV peak from ^{235}U and the 1001 keV peak from ^{234m}Pa (^{234}Th), following Eqn. 1.[1] where N^i = number of atoms of isotope i, $C(E)$ = peak area of gamma-ray j of energy E, $T_{1/2, i}$ = half-life of isotope i, BR_j = branching ratio of gamma-ray j, and $RE(E_j)$= relative efficiency value of gamma-ray j determined by a nonlinear least squares curve fit to the relative efficiency values at various energies. Thus, this method relies on the attainment of secular equilibrium between ^{238}U and ^{234}Th, unless the date of last chemical separation (in the case of UF_6, gas transfer) is known, in which case the code can make the appropriate correction. The software calculates a relative efficiency curve based on the measured gamma-rays and detector efficiency, as run in "physical efficiency" mode using eleven peaks from uranium isotopes and daughter products: 143, 163, 185, and 205 keV from ^{235}U and 258, 742, 766, 880, 883, 945 and 1001 keV from ^{234m}Pa, and requires no calibration.[4] The software can also be used in "planar" mode, which relies on low energy x-ray and gamma-ray peaks to quantify the isotopic fractions, however 30B cylinder walls are too
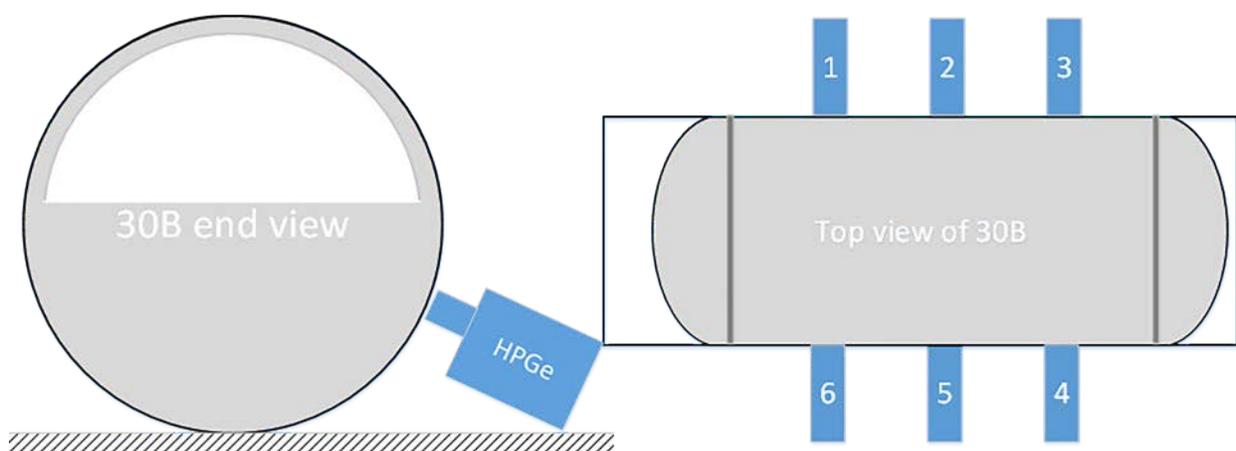
Figure 1: Geometry of the six position analyses around a 30B cylinder. The grey area is to suggest the expected distribution of UF_6 inside the cylinder.

thick for this method. The ratio of N^i and N^k is the enrichment as atom % but is converted by the software to weight % which is more commonly employed in the nuclear industry.

$$\frac{N^i}{N^k} = \frac{C(E_j^i)}{C(E_l^k)} * \frac{T_{1/2}^i}{T_{1/2}^k} * \frac{BR_l^k}{BR_j^i} * \frac{RE(E_l)}{RE(E_j)} \tag{1}$$

3. Results

To assess the accuracy of the measured apparent enrichment, the percent difference between the measured and declared weight% value was calculated following Eqn. 2.

$$\% \ difference = 100 * \frac{\left({}^{235}U_{measured} - {}^{235}U_{declared} \right)}{{}^{235}U_{declared}} \tag{2}$$

Six cylinders showed accurate, relatively constant uranium enrichments at all six positions around the cylinder, represented by calculated apparent enrichments within 20% of the declared value at all positions (**Fig. 2 left**). Three cylinders were found to have different apparent enrichments on

either side of the cylinder with side 1-2-3 showing one consistent apparent enrichment within 10% of the declared value, and side 4-5-6 showing a different apparent enrichment (**Fig. 2 right**).

The spectra were examined in Peak Easy v4.98.1 [8] to determine the count rates of the 185.7 keV peak from ${}^{235}U$ and the 1001 keV peak from ${}^{234m}Pa$. Count rates, relative to the live time, measured by five detectors in six positions around apparently heterogeneous cylinders are shown in **Fig. 3.** There was a correlation between slightly lower 185.7 keV count rate relative to the other side (~5% difference in count rate) and decreased apparent enrichments calculated as calculated by FRAM™ in these heterogeneous cylinders. Variations in 185.7 keV count rate by ~4% as a function of measurement position at the cylinder have been noted by Dufour et al. (2019) [9] so these slight variations in 185.7 keV count rate not significant. The 1001 keV peak count rates show large variation between the two sides of the heterogeneous cylinders, with the apparently low-enriched side showing up to 6x higher ${}^{234}Th-{}^{234m}Pa$ count rate (**Fig. 3**).
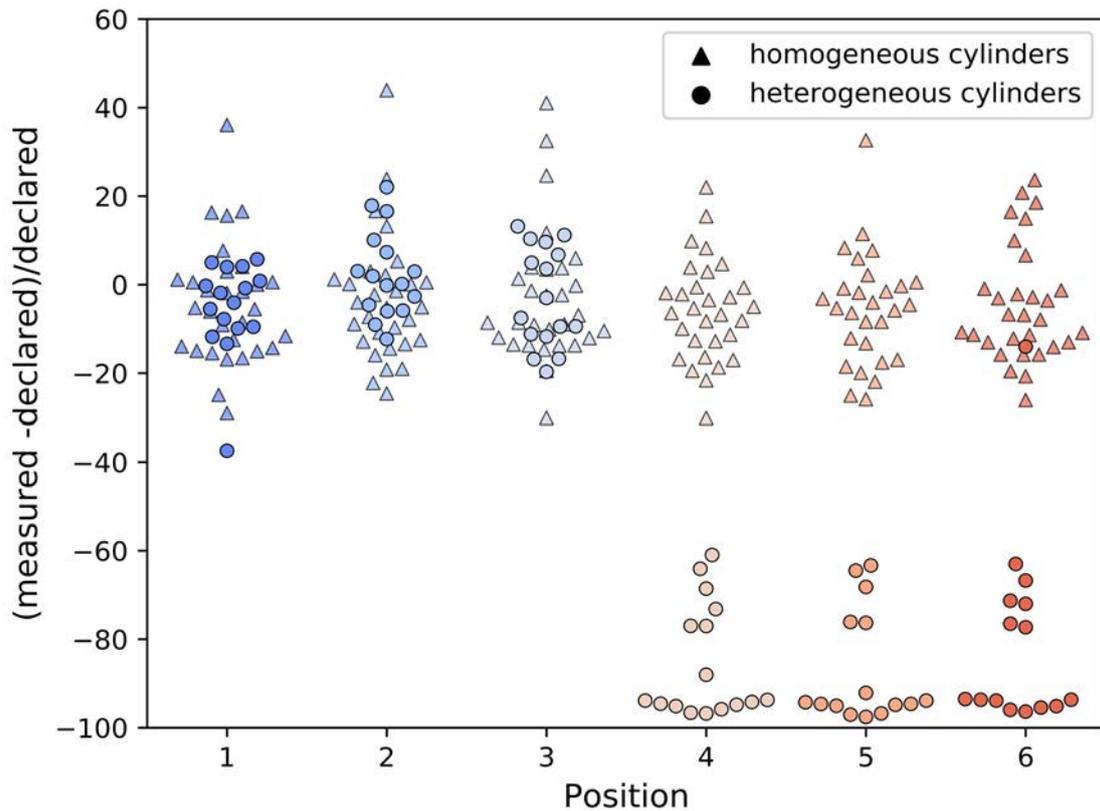
Figure 2: Accuracy of position analyses around the six "homogeneous" cylinders (triangles) and three "heterogeneous" cylinders (circles) plotted as the percent difference of the measured enrichment relative to the declared cylinder tag enrichment.
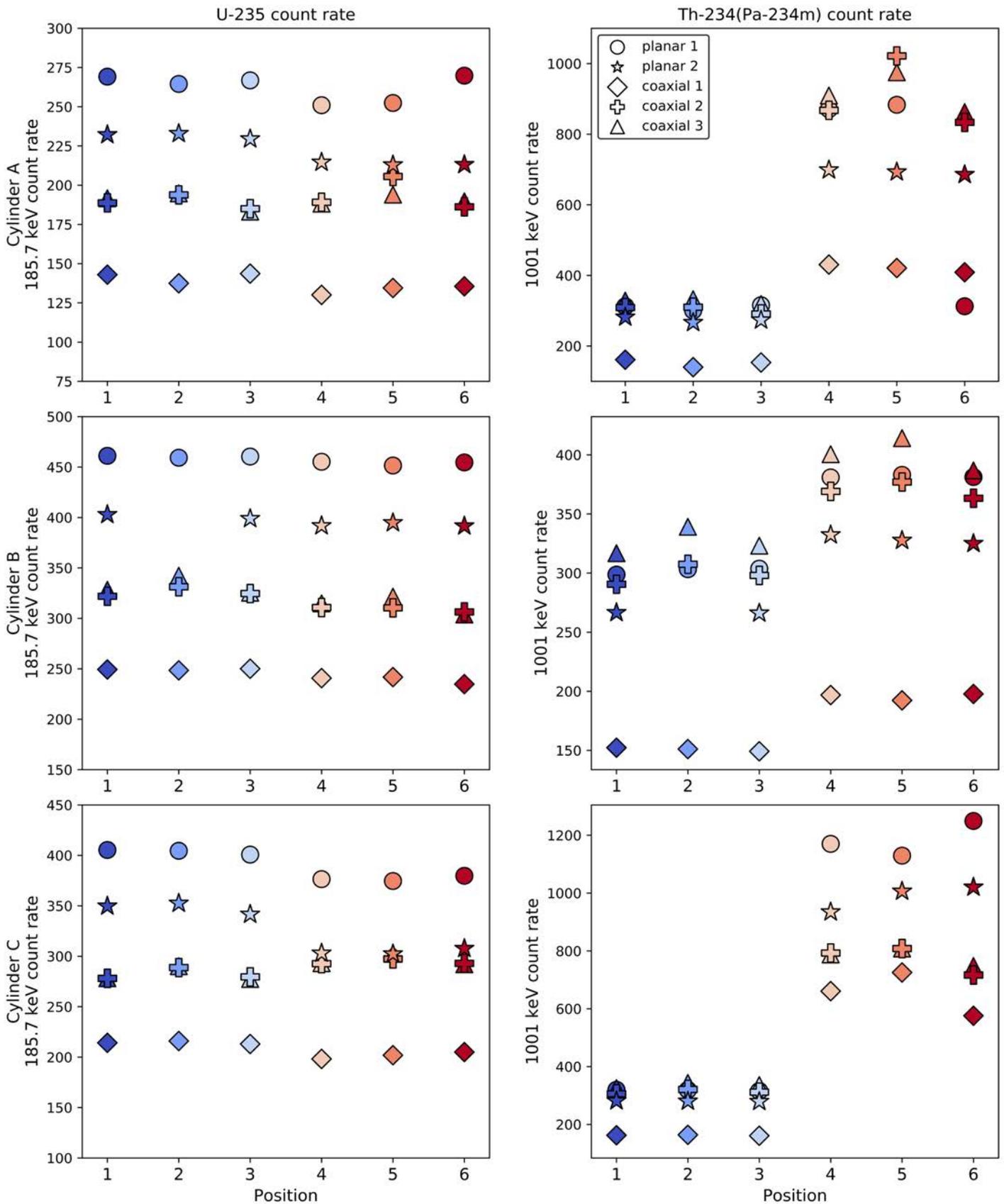
Figure 3: The deadtime corrected 185.7 keV peak count rate (left column) and 1001 peak count rate (right column) plotted by position, in counts per second, for three heterogeneous cylinders. Count rates for Cylinders A, B and C are groups in the top, middle and bottom plots, respectively. Markers denote five different detectors and colors correspond to position (1, 2, 3 = blues; 4, 5, 6 = reds). Measurements at positions 1, 2, and 3 produce accurate ^{235}U apparent enrichments while the measurements at positions 4, 5, and 6 shows apparent enrichment values that are consistently low. The Y-axis range varies because the three cylinders contain different U enrichments. Measurement uncertainty propagated from the total counts is within the data points.

4. Discussion

4.1 Detector performance

Because each detector was used at every position around the cylinder, these data can be used to evaluate detector performance without an added bias of position-dependence. When the homogeneous cylinders are considered, the planar detectors measure, on average, slightly more accurate uranium enrichments (**Fig. 4**). Using FRAM™ to calculate an enrichment, planar detectors average ± 9% accuracy while coaxial detectors average within ±13% accuracy, but the difference between planar and coaxial detector accuracy is not statistically significant (**Fig. 4**). Therefore, we conclude there are no significant differences in the accuracy of the enrichment calculated from spectra measured by planar vs. coaxial detectors and that "coaxial" mode on FRAM™ can be applied to either detector type. Given this, we can generally evaluate the effects of detector placement independently from detector performance.

4.2 Heterogeneous apparent enrichments on opposite side of the cylinder

Six of the cylinders analyzed at six positions showed no significant differences in apparent enrichment related to detector position. Data collected from all positions at these six cylinders showed a similar range of accuracy, as determined by the percent difference between the measured and declared enrichment (**Fig. 2 triangles**). However, three of the cylinders analyzed showed extremely different apparent enrichments related to detector position on each side of the cylinder (**Fig. 2 circles**). Disequilibrium effects between parent and daughter isotopes can be ruled out as the cause of low apparent enrichments, because all eight of these low-enriched cylinders were analyzed between 6 months and 3.5 years after their fill dates. It is therefore assumed that secular equilibrium has been attained on a whole-cylinder scale. While variations can be observed from heel deposits [10], they are not likely to be as systematic as observed in these studies. Thus, we propose that heterogeneous UF_6 and daughter product distribution within the cylinders caused the low apparent enrichment observed on one side of the cylinder. It is assumed that detector placement relative to the filling profile illustrated in **Fig. 1** would have captured a homogeneous UF_6-daughter mixture. However, given that UF_6 can sublime when heated, asymmetric solar heating of the cylinder could result in a heterogeneous UF_6 distribution. A cylinder oriented east –west in a storage yard is likely warmed to a greater degree on its southern side due to solar heating. This process could result in partial UF_6 sublimation and removal from the warmed side, leaving behind nonvolatile daughter nuclides like Th and Pa on the warmed side. The cylinder wall temperatures were not measured during this analytical campaign, so it is important to note that proposed sublimation from solar heating
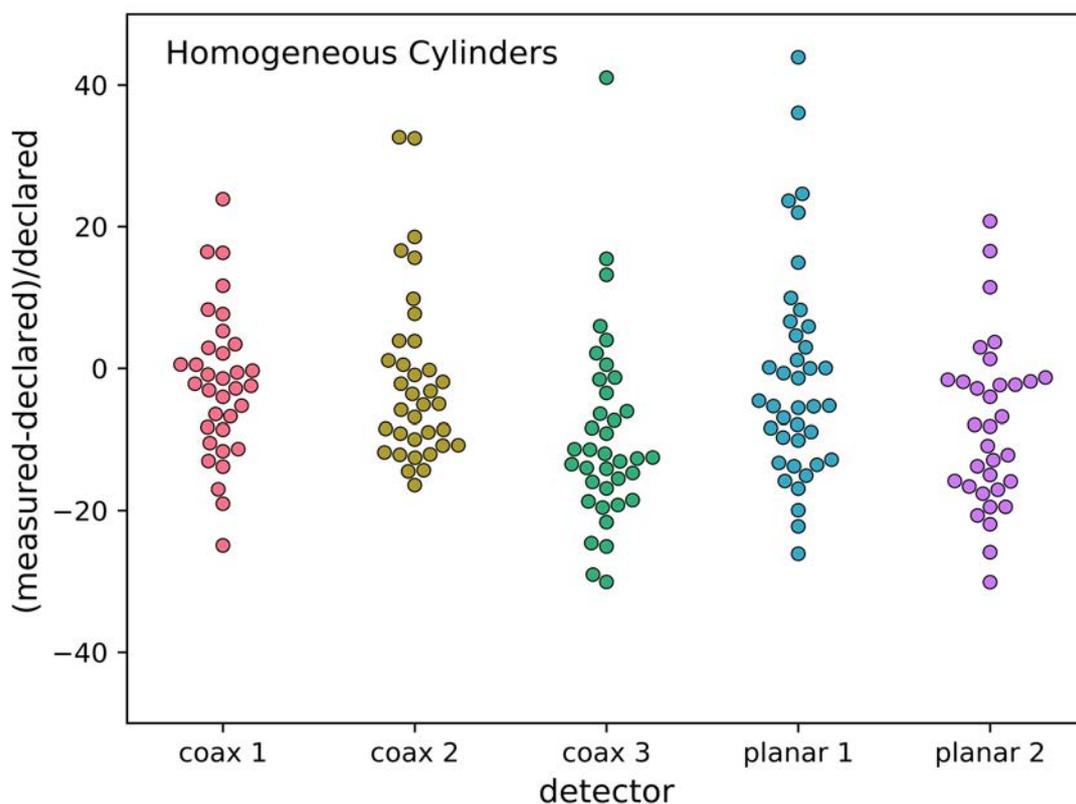
Figure 4: Accuracy of each detector for the six "homogeneous" cylinders plotted as the percent difference of the measured enrichment relative to the declared cylinder tag enrichment.

is only speculative, and further experiments should be completed to test this phenomenon.

The removal of parent U isotopes from the daughter Th products would result in localized disequilibrium between U and Th/Pa on the heated side of the cylinder. The added UF_6 to the cooler side would have minimal impact on the gamma-ray signal observed, as the 185.7 keV line would be self-shielded and the daughter nuclides would not provide significant contributions for months. However, the warmed side would likely have observable gamma-ray effects because UF_6 shielding was removed, allowing for a stronger daughter-product signal. This was observed in several cylinders analyzed here; **Fig. 3** compares the 185.7 and 1001 keV peak count rates at six positions around three cylinders. These cylinders were measured with five detectors, and each are plotted to show that the measured count rates were systematic across multiple detectors and not due to improperly tuned or faulty detectors. For each of these cylinders, positions 1, 2, and 3 show accurate apparent enrichments while positions 4, 5, and 6 show extremely low apparent enrichments. There is a clear 1001 keV peak count rate offset between each side of the cylinder; the low apparent enrichment side has a significantly higher 1001 count rate (**Fig. 3**). This is also true for the 766 keV peak from [234m]Pa, implying that the daughter product activity was measurably higher on the suspected warm side of the cylinder than on the cool side.

Additionally, there is a strong relationship between dead time and position. The majority of the spectra collected on the apparently low-enriched side (positions 4, 5, and 6) of the cylinders have exceedingly high dead times (>60% of the total count time), whereas all spectra collected on the "normally" enriched side (positions 1, 2, and 3) have dead times < 60% of the total count time (**Fig. 5**). These high dead times occurred in all detectors used. High dead times are presumably due to the relatively high daughter product activity. This would suggest that cylinders with significant dose differences between their sides may produce erroneous data on the side with higher dose readings, because dose generally correlates to the abundance of high activity [234m]Pa. Therefore, dose rate measurements and/or dead time monitoring could be used in the field to quickly identify potentially heterogeneous UF_6 distribution within cylinders.

4.3 Measuring spatial disequilibria within UF_6 cylinders

Because FRAM™ relies on a ratio between the 1001 keV peak and the 185.7 keV peak, it is sensitive to spatial homogeneity between parent U and daughter Th and Pa isotopes. This means FRAM™ calculates a lower apparent enrichment on the warm side as there is increased signal related to the high energy gamma-ray peak signal from [238]U. The traditional enrichment meter method is less susceptible to the effects of spatial disequilibria as it only uses the intensity of the [235]U peak; however, it is not totally immune. Data
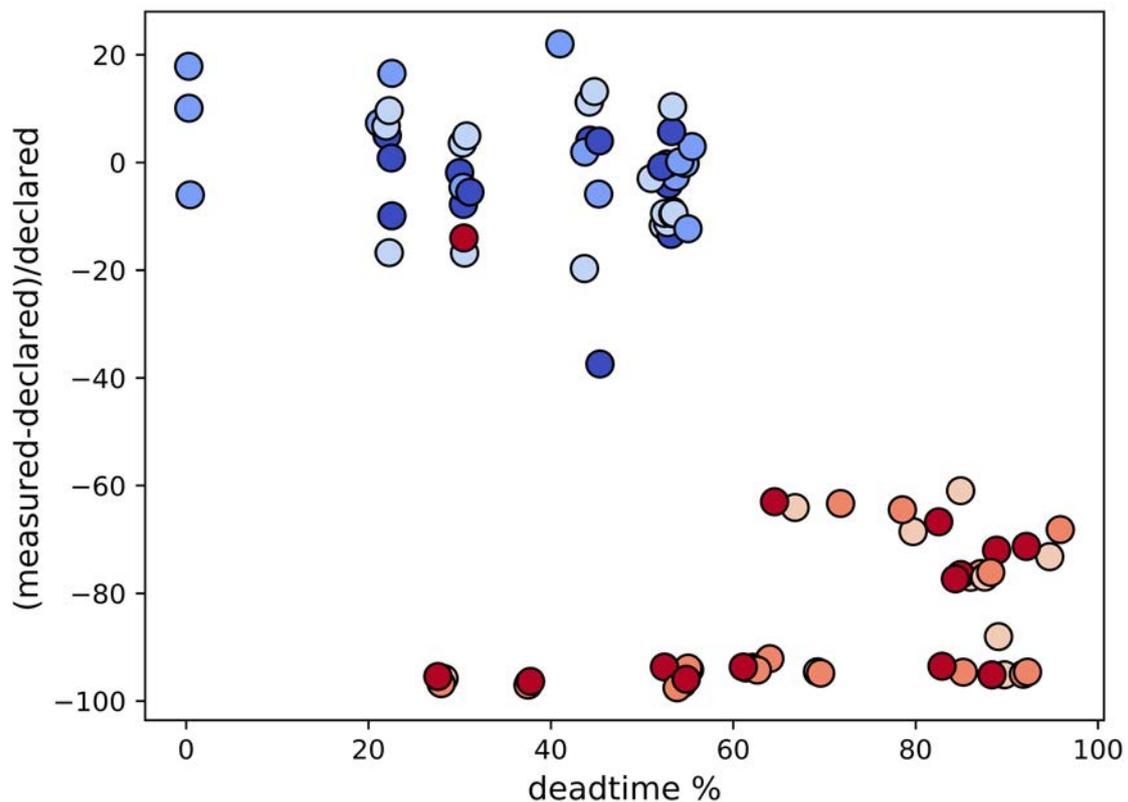
Figure 5: Dead time (% of total time) plotted against the accuracy of the [235]U enrichment measurement for the three heterogeneous cylinders. Accuracy is calculated as the percent difference between the measured and declared enrichments. Colors correspond to position (1, 2, 3 = blues; 4, 5, 6 = reds) as in previous figures.

in **Fig. 6** show a comparison between the spectra analyzed with FRAM™ and the 185.7 keV enrichment meter method for the three cylinders presented in **Fig. 3.** The enrichment meter was calibrated on two homogeneous cylinders from this facility with an enrichment of 4.95% and 0.71% ^{235}U. It was assumed that all wall thicknesses were the same, so no corrections were made for wall thickness. The results from the enrichment meter data treatment on the warmed side are much more accurate than the FRAM™ results but are still slightly depressed from the true enrichment (**Fig. 6**). As shown in **Fig. 3,** the 185.7 keV count rates are very similar between the two sides. This is likely because, although some UF$_6$ was suspected to be have been removed from the warm-side wall, a deposit that was close to infinite

thickness for the low energy 185.7 keV gamma-ray remained. Thus, the peak is only slightly altered by suspected material removal. Additionally, the higher dead times resulting from increased daughter product activity likely impacted the apparent enrichments calculated by the enrichment meter. Going forward, the possibility of heating-induced spatial disequilibria and its detection by different spectral analysis methods should be considered when using these methods in the field. Because the cause of the heterogeneities reported here is only speculative (i.e., we do not have confirmation that the heterogeneous cylinders were exposed to more sunlight than the homogeneous cylinders), further study of this phenomenon in laboratory and field settings is encouraged.
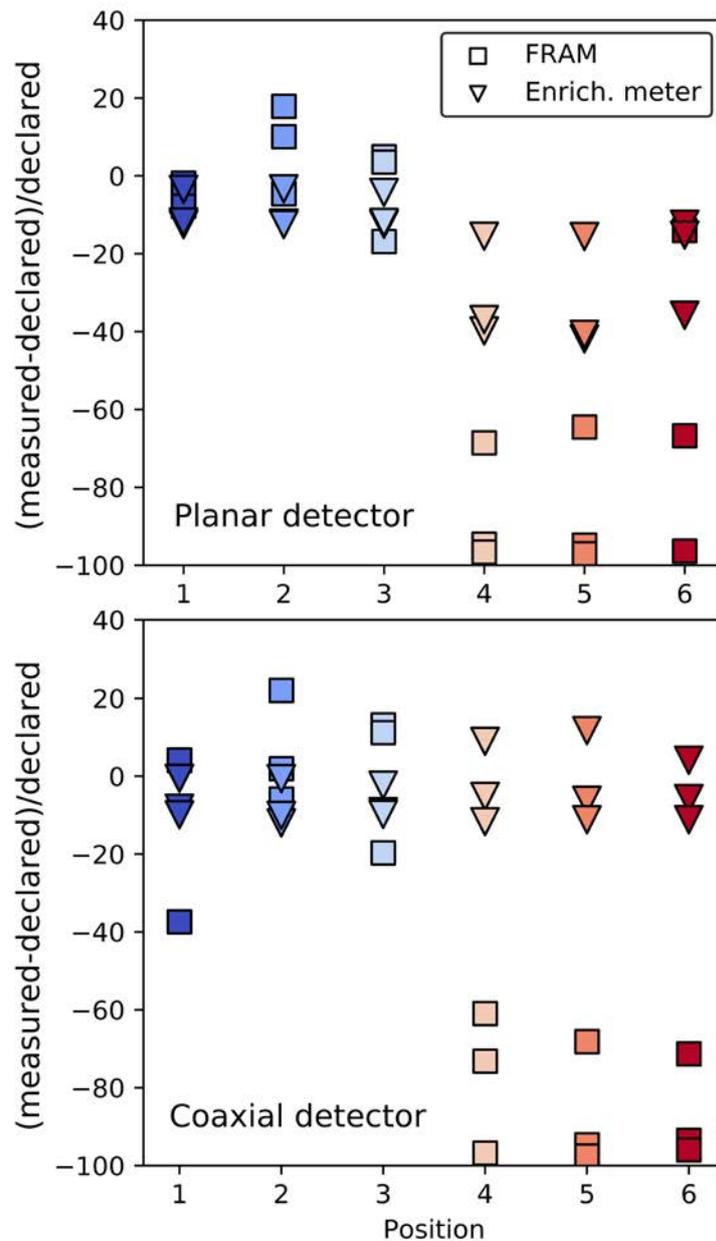
Figure 6: Comparison between FRAM™ (using peaks between 120 – 1010 keV) and the enrichment meter method (using only 185.7 keV) on heterogeneous cylinders. Data measured with two detectors from three heterogeneous cylinders are shown. Because FRAM™ relies on a ratio between the 185.7 and 1001 peaks, it is more sensitive to spatial disequilibria between UF$_6$ and its daughters in the cylinder. Colors correspond to position (1, 2, 3 = blues; 4, 5, 6 = reds).

5. Conclusions

The application of FRAM™ to determine enrichment of UF_6 in thick-walled cylinders can be performed with similar accuracy using either planar or coaxial detectors. However, caution should be exercised when applying FRAM™ or other enrichment meters that require the use of uranium daughter isotopes for measurements on UF_6 cylinders, especially if there are significant discrepancies between deadtime and/or dose rates at different locations around the cylinders. Cylinder placement within a storage yard should be noted when measurements are made, and if uneven solar heating is suspected, measurements should be taken at multiple points around a cylinder to assess the accuracy of the uranium enrichment measurement. Further studies are needed to assess the effects of solar heating on UF_6 distribution within a cylinder.

6. Acknowledgements

7. References

[1] Sampson, T. E.; Kelly, T.A. "PC/FRAM: a code for the nondestructive measurement of the isotopic composition of actinides for safeguards applications" *Appl. Radiat. Isot*. 1997, 48, 1543–1548.

[2] Sampson, T. E.; Verrecchia, G. P. D.; Swinhoe, M. T.; Schwalbach, P.; Gustafsson, J.; Anderson, A. M.; Myatt, J.; Metcalfe, B. "Test and Evaluation of the FRAM Isotopic Analysis Code for EURATOM Applications," *Annu. Meet. Proc. Inst. Nucl. Mater. Manage*., July 25-29, 1999, Phoenix, Arizona.

[3] Vo, D. T.; Sampson, T.E. "Methods for uranium isotopic analysis with the FRAM isotopic analysis code", *Annu. Meet. Proc. Inst. Nucl. Mater. Manage*., July 25-29, 1999, Phoenix, Arizona.

[4] Vo, D. T.; Sampson, T.E. FRAM Version 5, User Manual, 2011, Los Alamos National Security, LLC (2011)

[5] Berndt, R.; Franke, E.; Mortreau, P. "[235]U enrichment or UF_6 mass determination on UF_6 cylinders with non-destructive methods" *Nucl. Instrum. Methods A*, 612 (2010) 309–319.

[6] Greaney, A. T.; Smith, S. K.; Venkataraman, R.; Richards, J. M.; Fugate, G.A. "Comparison of Gamma-Ray Spectral Analysis Methods for Thick-Walled UF_6 Cylinders" *Nucl. Instrum. Methods A*, 2020, 977, 164291

[7] Greaney, A. T.; Smith, S. K.; Venkataraman, R.; Richards, J. M.; Fugate, G.A. "Applications of HPGe-detected high energy gamma rays toward quantifying neutron emission rates and [234]U enrichment in UF_6 cylinders" *Nucl. Instrum. Methods A*, 2020, 163912

[8] Rooney, B.; Garner, S.; Felsher, P.; Karpius, P. PeakEasy 4.98, 2018, Los Alamos National Laboratory, Release LA-CC-13-040.

[9] Dufour, J.-L.; Pepin, N.; Deyglun, C.; Weber, A.-L. "Optimisation and uncertainty estimation of the enrichment meter measurement technique for UF6 cylinders", *ESARDA Bull*., 2019, 59, 2-10.

[10] McFerran, N.; Canion, B.; McDonald, B.; Kulisek, J.; Dreyer, J.; Labov, S.; Enqvist, A. "Gamma-ray spectrum variations for surface measurements of uranium hexafluoride cylinders" *Nucl. Instrum. Methods A*, 2020, 961, 163675.